

# The Effect of Various Types of Constant and Time Dependent Heating on Human Tissue: A Finite Element Approach

Mridul Sannyal\* and Abul Mukid Md. Mukaddes

Department of Industrial and Production Engineering, Shahjalal University of Science and Technology, Sylhet-3114, BANGLADESH

Received: May 31, 2020, Revised: June 29, 2020, Accepted: June 30, 2020, Available Online: July 01, 2020

## ABSTRACT

Cancer is one of the most leading causes of death now worldwide. Most of the cancer therapy aims to raise the temperature of the cancerous tissue above a therapeutic value and thermally kill or destroy it. Minimizing the damage of the healthy cells surrounding the infected cells is one of the major concerns of these therapies. Precise acknowledgment of the temperature profile of living tissue during therapy is of utmost necessity for this purpose. Towards that direction, this paper presents an unsteady finite element model of the bioheat equation to analyze the temperature distribution during the thermal therapy. A C language based system has been developed to solve the unsteady part of the problem employing Crank-Nicolson method and to solve the linear problem employing the Gauss elimination technique. Using this system, we investigate thermal behaviors in human tissues subjected to constant, sinusoidal spatial and surface, point, and stochastic heating. It was found that surface heating is beneficial for treating skin surface cells, while laser heating for the cells that lie below the skin surface. Moreover, for deep cell, the point heating style can bring the most desirable outcome. Results describe in this paper could be useful for researchers and doctors to optimize the treatment procedure, even protocols.

Keywords: FEM; Bioheat Transfer; Human Tissue; Pennes Equation; Spatial Heating.



This work is licensed under a [Creative Commons Attribution-NonCommercial 4.0 International](https://creativecommons.org/licenses/by-nc/4.0/)

## 1. Introduction

Prior acknowledgment of the temperature distribution of thermal therapy could help optimize treatment procedures and take necessary precautions for probable danger during therapy. Undoubtedly experimental study is most welcome in this field. However, as human subject involves, the experimental approach often became very difficult to perform and result in a hazardous situation. Moreover, it is time-consuming and needs costly equipment setup. Hence mathematical modeling is preferred in that area instead of clinical trials. But the complexity of modeling biological systems and treatment procedures makes it so tough in practice even impossible. That's why computational modeling of the biological bodies has received considerable attention in the research community in the past decade. Rapid advancement in computational technology, which enables better accuracy with less computational cost, added a new era to this progress. Moreover, due to its simplicity in use and low cost, it is widely used in simulation of biomedical problems. With the help of computer technology and mathematical model, it is possible to calculate and visualize the stationary and transient temperature inside biological bodies during thermal therapy.

Heat transfer in living tissue has become a very interesting topic for scientists and engineers because of its broad application in bioengineering and designing of medical protocols. Many therapeutic applications need the proper thermal description of the human body. Not only that, but many medical operations also rely on engineering methods to determine the safety and risk level involved in many surgeries. At present, mathematical modeling of Bioheat transfer is widely used in treating tumors, cryosurgery, laser eye surgery, and many other applications. The

success of hyperthermia treatment much depends on the proper knowledge of heat transfer in blood perfused tissue [1]-[2].

Over the years, several mathematical models have been developed to describe the heat transfer within living biological tissues. The most widely used bio-heat model was introduced by Pennes in 1948 [3]. Pennes Bio-heat-equation has been widely used to approximate the overall temperature distribution in tissue. The Pennes model was initially used to predict the temperature distribution in the human forearm. Due to its simplicity (uniform thermal conductivity, blood perfusion, and metabolic heat generation), it was implemented in various biological research work such as for cancer hyperthermia, cryosurgery etc. Therefore, to obtain a flexible solution that can solve similar problems is very desirable. Reports on the analytical and numerical solutions of the bio-heat transfer problem are found in the literature. In some analytical cases, sinusoidal heat flux [4] and sometimes cooling of the skin [5] were considered as boundary conditions. In some numerical analysis, sinusoidal surface heat flux was used as boundary condition [6]. Researches related to the bio thermos- mechanical were reviewed in [7]. Monte Carlo method was used to solve the multidimensional problem in [8]. The result of boundary element method and finite element method for the numerical solution of the steady state bio-heat transfer model of the human eye were compared in [9]-[10]. The finite element method was used for the thermal-magneto static analysis in biological tissues in [11]. Some commercial software includes bio-heat transfer functions with limited boundary conditions. It is quite difficult to have the temperature profile of a particular point or a line within the biological tissue with different time intervals using that software. The development of a free finite element code of bio-heat

equations can meet the purpose. The objective of this research is to develop a one dimensional finite element code for the solution of both steady and transient bio-heat equation. The popular Crank-Nicolson method was used in time discretization of the transient analysis. The developed finite element code was used to simulate the thermal response of tissue during cancer hyperthermia, laser surgery, tissue heating with a hot disk, and point heating. Moreover, time-dependent spatial and surface heating were incorporated. The effect of surface heating, step heating, sinusoidal heating, and point heating was thoroughly investigated. The temperature profile for all cases is found with valuable information for the physicians and researchers.

## 2. Bio Heat Transfer

For the study of bio-heat transfer in human tissue, the most useful one is Pennes equation which can be expressed as

$$k \frac{\partial^2 T}{\partial x^2} + \omega_b \rho_b c_b (T_a - T) + Q_m + Q_r = \rho c \frac{\partial T}{\partial t} \quad (1)$$

For steady state case the Eq. 1(a) is reduced as

$$k \frac{\partial^2 T}{\partial x^2} + \omega_b \rho_b c_b (T_a - T) + Q_m + Q_r = 0 \quad (2)$$

Where  $\rho$ ,  $c$ ,  $k$  are respectively the density, the specific heat, and the thermal conductivity of the tissue;  $\rho_b$ ,  $c_b$  denote density, and specific heat of blood, respectively. The  $\omega_b$  is the blood perfusion,  $T_a$  the known arterial temperature, and  $T(x, t)$  is the unknown tissue temperature. Where  $Q_m$  is the metabolic heat, and  $Q_r(x, t)$  is the heat source due to spatial heating.

Let the one dimensional problem of length  $L$ , where the skin surface is defined at  $x = 0$  and the body core at  $x = L$ . The constant body core temperature is defined as  $T_c$ ,  $h_0$  is the ambient heat convection coefficient between the skin surface and the surrounding air and  $T_0$  is the ambient temperature. At the skin surface ( $x = 0$ ), the thermoregulation between the skin and ambient air is governed by the thermal convection between air and skin. While as the tissue temperature remains constant within a narrow limit, i.e., 2-3 cm, the boundary conditions at the body core is considered as temperature boundary conditions. Thus the boundary conditions for this particular 1-D problem can be written as:

$$-k \frac{\partial T(x)}{\partial x} = -h_0 [T_0 - T(x)] \quad \text{at } x = 0 \quad (3)$$

$$T = T_c \quad \text{at } x = L \quad (4)$$

In some cases, force convection cooling is applied at the skin surface to remove excessive heat from the skin surface, in such case the boundary condition at the skin surface is defined as

$$-k \frac{\partial T(x)}{\partial x} = -h_f [T_f - T(x)] \quad \text{at } x = 0. \quad (5)$$

In some cases, the boundary condition is time dependent. So time dependent boundary conditions can be expressed as

$$-k \frac{\partial T(x)}{\partial x} = Q(t) \quad \text{at } x = 0. \quad (6)$$

Here  $Q(t)$  is the time dependent heat flux.

### 2.1 Finite element discretization

The first step of the finite element discretization is to develop a weak form that is a weighted integral statement and

is equivalent to both the governing differential equation as well as a certain type of boundary condition. The simplest form of the Eq. (1) is

$$k \frac{\partial^2 T}{\partial x^2} - BT + q = \rho c \frac{\partial T}{\partial t} \quad (7)$$

Where  $B = \omega_b \rho_b c_b$  and  $q = BT_a + Q_m + Q_r$ . The weak form of the differential equation (applying the Weighted Residual method) is derived as

$$\int_{x_a}^{x_b} [W \rho c \frac{\partial T}{\partial t} + k \frac{\partial T}{\partial x} \frac{\partial W}{\partial x} - BWT - Wq] + (WQ)_{x_a} + (WQ)_{x_b} = 0 \quad (8)$$

Where  $W$  is the weighted function, and  $Q$  is the secondary variable. A linear element is considered in this model whose temperature function is expressed as

$$T_h^e(x) = \sum_{j=1}^2 \varphi_j^e(x) T_j^e \quad (9)$$

Using the linear approximation of Eq. (9) finally a linear system was derived of the following form

$$[C]\{\dot{T}\} + [K]\{T\} = \{q\} + \{Q\} \quad (10)$$

Where  $C$  is the capacitance matrix,  $K$  is heat conductive matrix and  $T$  is unknown temperature and others are known vectors.

### 2.2 Time Discretization Scheme

A simple time integration scheme for the Eq. (10) is derived by assuming that  $C$  and  $K$  are constant. In such case, the matrix differential equation can be discretized with response to time as

$$C \frac{T^{n+1} - T^n}{\Delta T} + \alpha K T^{n+1} + (1 - \alpha) K T^n = Q + q \quad (11)$$

Where  $T^{n+1}$  and  $T^n$  are the vectors of unknown nodal values at times  $n\Delta T$  and  $(n + 1)\Delta T$ , respectively and  $\alpha$  is the weighting factor. The  $\alpha$  must be chosen in the interval between 0 and 1. When the value of  $\alpha$  is considered 0.5, the process is called the popular Crank-Nicolson method. The discretized Eq. (11) can be written as:

$$\left(C \frac{1}{\Delta T} + \alpha K\right) T^{n+1} = \left[C \frac{1}{\Delta T} - (1 - \alpha)K\right] T^n + Q + q \quad (12)$$

The Eq. (12) was solved using an iterative procedure. The initial temperature is known and then the temperature of the next step is calculated from the solution of Eq. (12) through the Gauss elimination technique.

### 2.3 Boundary Conditions and Input Parameters

Throughout the study at  $X=L$ , the temperature boundary condition is used.

However, depending upon the types of heating boundary condition (3), (5) and (6) is used at  $X=0$ .

In section 3.2, 3.3, 3.8, and 3.9 boundary condition (3) is used at the skin surface. Heat flux boundary condition Eq. (6) is used in sections 3.4 and 3.5 at  $X=0$ . Where the force convection boundary condition Eq. (5) is used in sections 3.6 and 3.7. The input parameters used in this study is summarized in [Table 1 \[12\]](#).

**Table 1** Input Parameters.

Parameters	Value
Thermal conductivity (k)	0.5 w/m <sup>2</sup>
Convection Coefficient (h <sub>o</sub> )	10 w/m <sup>2</sup>
Forced convection coefficient (h <sub>f</sub> )	100 w/m <sup>2</sup>
Environmental Temperature (T <sub>0</sub> )	25 °C
Temperature of the Artery (T <sub>a</sub> )	37 °C
Body core temperature (T <sub>c</sub> )	37 °C
Metabolic heat generation (Q <sub>m</sub> )	33800 w/m <sup>2</sup>
Density of blood (ρ <sub>b</sub> )	1000 kg/m <sup>3</sup>
Density of tissue (ρ)	1000 kg/m <sup>3</sup>
Specific heat of blood (c <sub>b</sub> )	4200 J/kg.°C
Specific heat of tissue (c)	4200 J/kg.°C
Blood perfusion (ω <sub>b</sub> )	0.0005 ml/s/ml

**3. Results and Discussion**

For the simple thermal analysis, from the skin surface to tissue body is enough to consider. So to avoid the computational complexity, a 1D tissue of length (L) of 30 mm is considered as a computational model.

**3.1 Code Verification**

**Fig. 1** shows a comparison between numerical result and the analytical result obtained from [12] for the steady state case considering the Eq. (3-6). The comparison shows a better agreement. The boundary conditions are defined as describe in Eq. (3) and Eq. (4).

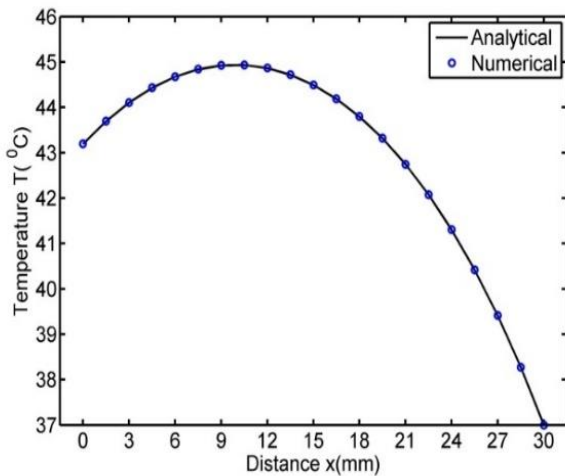


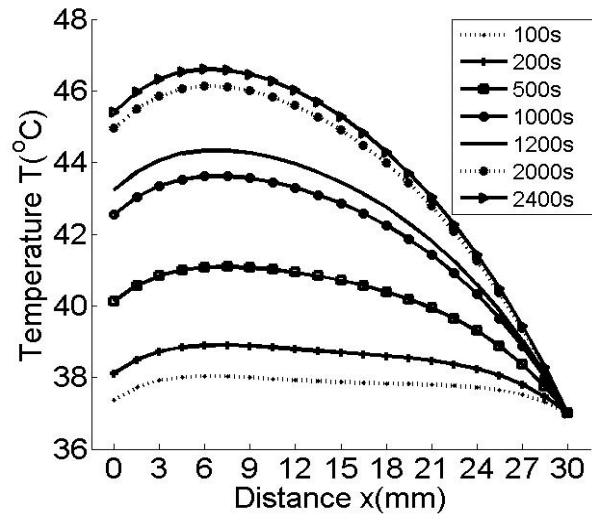
**Fig. 1** Comparison with analytical solution.

This figure shows that initially, tissue temperature increases along with distance due to metabolism, but after attaining the highest value, it decreases towards the body core as temperature boundary condition is applied to the body core. Here the maximum temperature is 45°C, which is located about 11 mm below the skin surface.

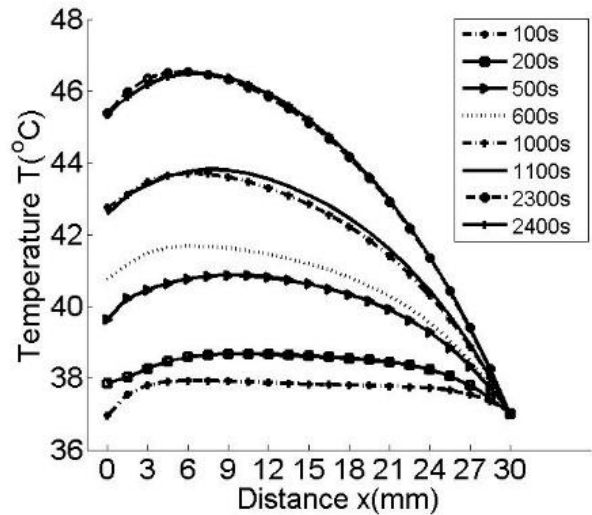
**3.2 Spatial Heating**

Laser and microwave therapy are some of the most widely used non-invasive techniques to destroy malignant cells. In this section, we aim to know the temperature distribution of human tissue during heating by laser or microwave.

In case of heating by laser and microwave, the heat absorption rate can simply be approximated by Beers Law, which can be expressed as  $Q_r = \eta P_o(t)e^{-\eta x}$  in which heat flux decays exponentially with respect to distance from the skin surface [13]-[15]. Here  $P_o(t)$  is the time-dependent heating power on the skin surface, and  $\eta$  is the scattering coefficient. Since  $P_o(t)$  and  $\eta$  vary from one apparatus to another, so it is important to know the influence of these parameters on tissue temperature.  $P_o(t)$  can be either constant and time-dependent. In our study, we have considered both cases.



(a)



(b)

**Fig. 2** Temperature distribution at different times; ( $\eta = 200 \text{ m}^{-1}$ ), (a)  $P_o(t) = 250 \text{ W/m}^2$ , (b)  $P_o(t) = 250 + 200\cos(0.02t) \text{ W/m}^2$ .

**Fig. 2** depicts the transient temperature at different times when tissues subject to two different spatial heating. **Fig. 2 (a)** shows the case of constant spatial heating and while **Fig. 2 (b)** is for sinusoidal spatial heating. In both cases, at the early stage, the tissue temperature increases along with the distance from the skin surface due to external heating, but later it decreases towards the body core. Moreover, there is an inter-cross

between temperature curves at different times in Fig. 2 (b), which indicates the oscillation of the temperature inside the tissue due to sinusoidal spatial heating. These figures also reveal that the temperature within the tissue increases along with time and finally reached the steady state condition. Here the maximum temperature is about 47°C, and that lies 7 mm below the skin surface.

### 3.3 Effect of Scattering Co-efficient

Fig. 3 shows the effect of the scattering coefficient, where Fig. 3 (a) shows the result for constant heating, and Fig. 3 (b) depicts the result for sinusoidal heating. In both cases, the larger coefficient results in a higher temperature. Moreover, in the case of sinusoidal spatial heating, the larger coefficient returns higher amplitude. Fig. 3 (b) indicates the sinusoidal effect. Fig. 3 (a) shows that after about 3000 seconds (approximately), tissue temperature begins to stabilize.

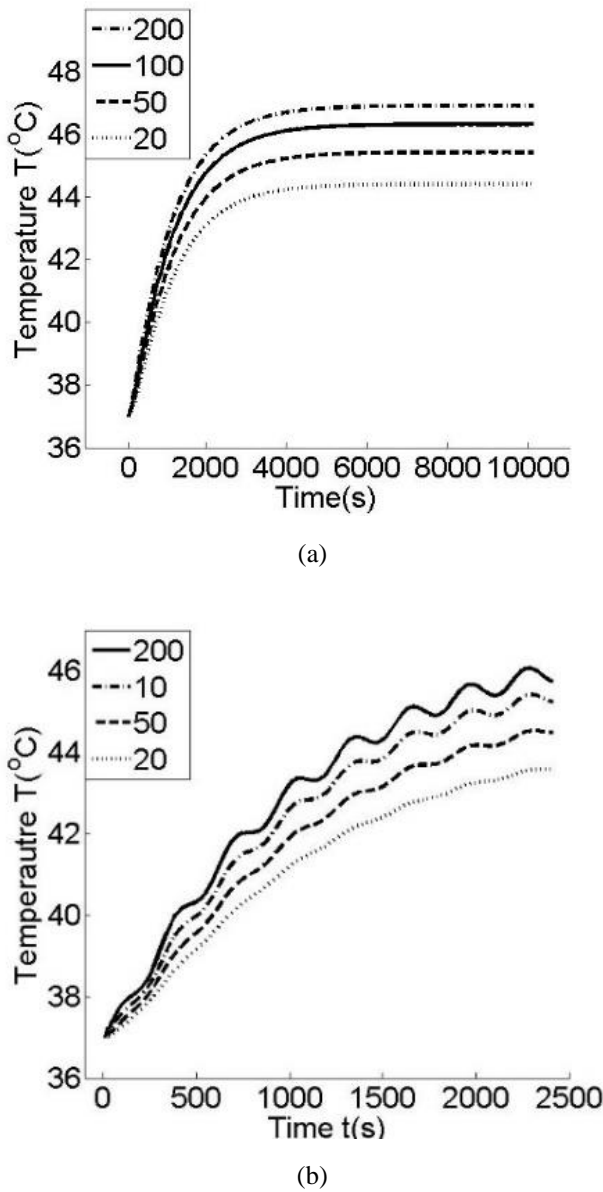


Fig. 3 Effect of scattering coefficient on temperature response at skin surface ( $f(t) = 0$ ); (a)  $P_o(t) = 250 \text{ W/m}^2$ ; (b)  $P_o(t) = 250 + 200\cos(0.02t) \text{ W/m}^2$ .

### 3.4 Surface Heating

Heating with a hot plate or pad is a traditional approach to retain from pain. Depending upon the temperature and thermal properties of heating disk, this approach can be used for cell repair or to destroy affected cells. In this section, we analysed the thermal behaviour of living tissue subjected to time-dependent surface heat flux. Both constant and step heating are considered in this study. In constant heating, human tissue is heated with a heating pad at a constant rate. In step heating after heating for a certain period heat source is removed and allows it to cool. Results are calculated at different heat flux and time. Here Eq. 3(a) is used for skin surface boundary conditions.

*Constant Heating:* The calculated tissue temperature for constant surface heating is shown in Fig. 4 (a) at different heat flux. And skin temperature at different times, along with the distance from the skin surface, is shown in Fig. 4 (b). From Fig. 4 (a) higher heat flux results in a higher temperature, and temperature increases as time increases. At the early stage, temperature increases rapidly, but as time increases, increasing rate decreases and tends to be stabilized. From Fig. 4 (b) it is clear that temperature decreases towards the body core.

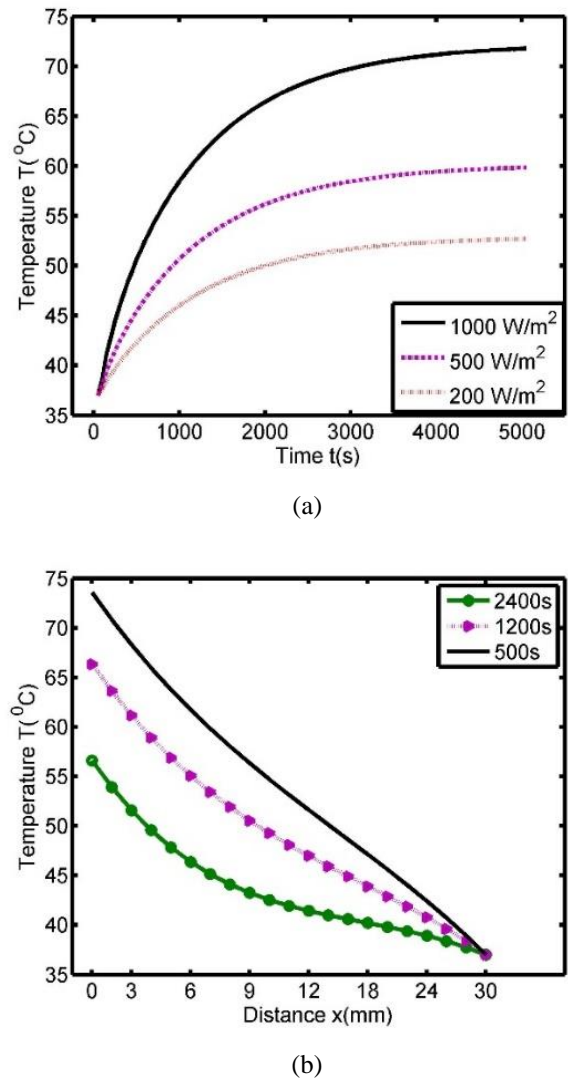
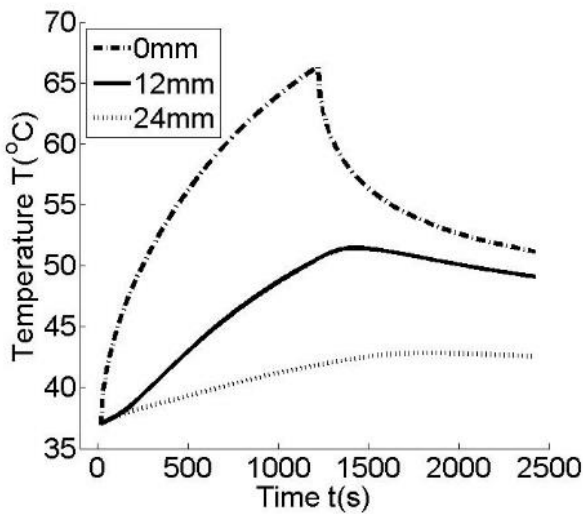


Fig. 4 Effect of surface heat flux to the skin surface temperature response.

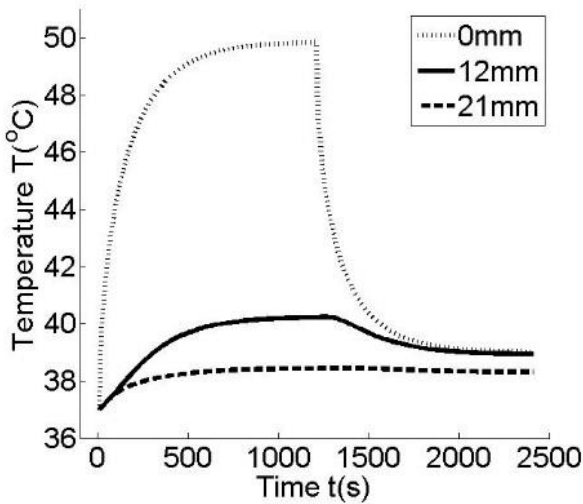
*Step Heating:* In this case, after heating for 1200 seconds the heat source is removed. In this section, temperature distribution at three different locations is obtained over time. It is very useful in eye surgery via a single laser pulse due to a flash fire, heating using a hot plate for a short period of time [10]. The heating power used in this particular type of investigation is expressed as

$$Q(t) = \begin{cases} 1000 \frac{w}{m^2}, & t \leq 1200 \text{ s} \\ 0 \frac{w}{m^2}, & t > 1200 \text{ s} \end{cases} \quad (13)$$

The transient temperature at three different locations of the skin is shown in Fig. 5. Where  $Q_r=0$ , in Fig. 5. The result also carried out for two different value of blood perfusion  $\omega_b=0.0005 \text{ ml/s/ml}$  and  $\omega_b=0.004 \text{ ml/s/ml}$ .



(a)



(b)

**Fig. 5** Transient temperature at three positions ( $Q_r=0$ ): (a)  $\omega_b=0.0005 \text{ ml/s/ml}$ ; (b)  $\omega_b=0.004 \text{ ml/s/ml}$ .

Both figures show that as time increases, temperature also increases, but after 1200 seconds when the heat source is removed, tissue temperature decreases as time passes. Moreover, these figures show us the effect of blood perfusion

in surface heating. Also the higher blood perfusion results in lower temperature and quick temperature loss (after 1200 seconds when  $Q(t)=0$ ). This happens as a higher blood flow rate carried away excess heat. Such information is valuable in thermal comfort analysis. In practice, the temperature of the surrounding fluid temperature and duration should be in the safe range. A high temperature or long durable process may encounter pain, even burning of the skin.

### 3.5 Effect of Heating Frequency and Blood Perfusion

The calculated result for different heating frequency and blood perfusion is shown in Fig. 6 subjected to sinusoidal surface heating. The sinusoidal heating at the skin surface can be expressed as

$$Q(t)=q_0+q_w \cos(\omega_1 t) \quad (14)$$

Where  $q_0$  and  $q_w$  are the constant terms, and the oscillation amplitude of sinusoidal heat flux and  $\omega_1$  represents the heating frequency.

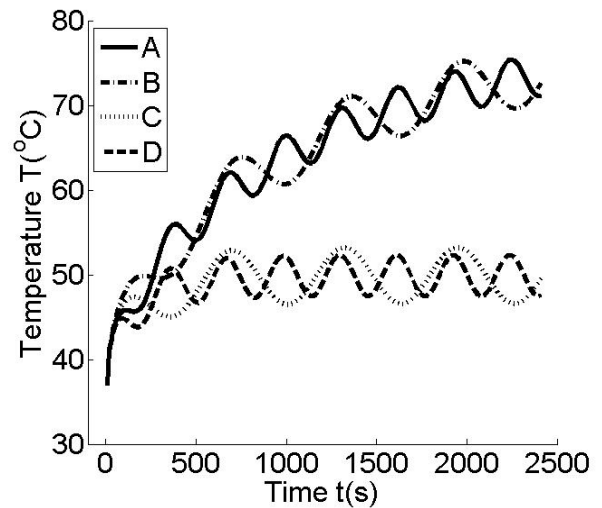


**Fig. 6** Effect of heating frequency and blood perfusion on sinusoidal surface heat flux.

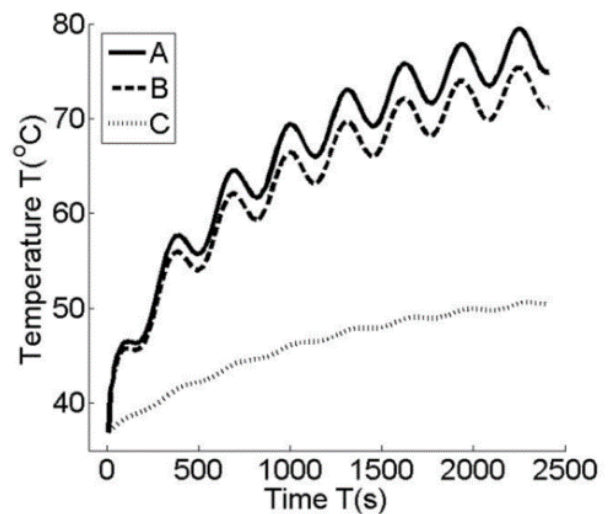


**Fig. 7** Different heating condition and its impact on skin surface temperature.

In Fig. 6 curves A and B, we use blood perfusion as 0.0005, where in curve C & D it is 0.004. While in curve A and C, we use a heating frequency of value, 0.02 were in B & D, it is 0.01. From these figures, we can say that high blood perfusion results in lower temperatures where temperature response under two different heating frequencies almost negligible.

The calculated tissue temperature result subject to simultaneously surface and spatial heating is shown in Curve A of Fig. 7. While Curve B represents a single sinusoidal surface heating ( $Q_r=0$ ), and curve C represents only sinusoidal spatial heating ( $f_1(t)=0$ ). The applied surface and spatial heating are  $Q(t)=1000+500\cos(0.02t)$  W/m<sup>2</sup> and  $P_o(t)=250+200\cos(0.02t)$ .

However, Fig. 8 illustrates the impact of frequencies of surface heating. Here the applied surface and spatial heating are  $Q(t)=1000+500\cos(0.02t)$  W/m<sup>2</sup> and  $P_o(t)=250+200\cos(0.01t)$  respectively. In curve A, we applied simultaneously sinusoidal surface and spatial heating. Curve B represents a single sinusoidal surface heating ( $Q_r=0$ ) when curve C represents only spatial heating ( $f_1(t)=0$ ).

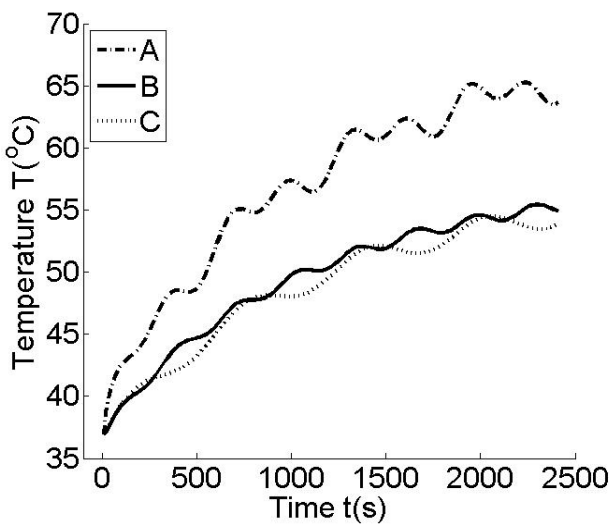


Fig. 8 Temperature distribution at different heating frequency.

In curve A of Fig. 8, the frequency of surface heating and spatial heating was the same, and thus, due to the same frequency, the resultant temperature appears having the same frequency as external heating. However, in curve A of Fig. 8, different heating frequency was applied to spatial and surface heating; that's why irregular frequency has appeared in tissue temperature.

### 3.6 Impact Forced Convection Boundary Condition

In this section, we concentrate on temperature profiles under different kinds of surrounding medium classified by their temperature. Fig. 9 depicts the tissue temperature distribution under different cooling medium temperature. Here force cooling significantly reduces the skin surface temperature. Moreover, lower cooling medium temperature results in lower skin surface temperature. However, the effect of forced cooling is negligible for the deep tissues, as shown in Fig. 9, the

temperature of the cells over approximately  $x=12$  mm line remains changeless for different cooling temperature.

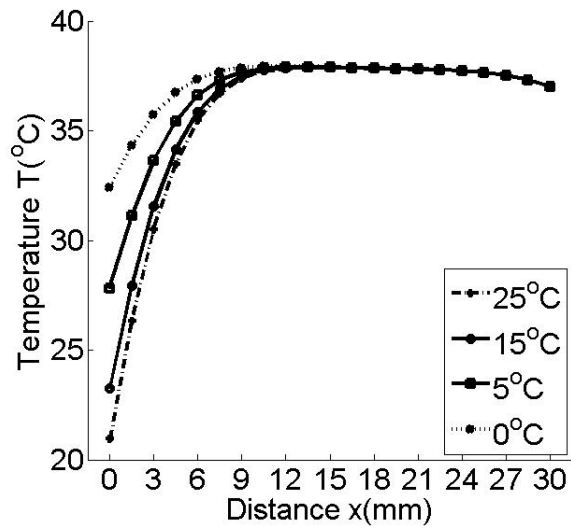


Fig. 9 Influence of cooling medium temperature on tissue temperature.

Using a cooling medium on the skin surface may be a good approach during hyperthermia treatment as it can reduce the skin temperature even below the core temperature, which may result in hypothermia. Hence, concentration should be given selecting proper cooling medium. Here the force convection coefficient of the cooling medium is considered as 100 W/(m<sup>2</sup>. °C).

### 3.7 Point Heating

Treating deep tumors- located at kidney, lung, or rectum- it is very difficult to adopt surgical treatment. In such a case, point heating can be an alternative to surgery due to its ability to treat a tumor with a defined volume. In such a case, the total heating power is deposited at the tumor site with the help of a microwave probe, radio-frequency probe etc. In this heating type, the target region is heated more than 50°C within few minutes. This heating is very beneficial in the case of thermal ablation when a target tissue is destroyed, injecting thermal energy at the tumor site [5],[6]. There is an inverse relationship between elevated temperature and exposure duration. For the same amount of tissue necrosis, the high temperature needs low exposure duration. On the contrary, the low temperature needs high exposure duration. So for effective treatment, we need to know the required temperature and exposure duration precisely. Moreover, in some cases, to protect the skin surface cells from excess heat, the cooling medium is used on the skin surface during treatment, which is a very efficient approach to reduce the skin surface temperature. In this investigation, we calculate the tissue temperature at different times, cooling medium properties, and heating power. To deposit total heating power at the desired site, we use the expression of the external heating as [12],[13].

$$Q_r(x,t)=P_1(t)\delta(x-x_0) \tag{15}$$

Where  $P_1(t)$  is the point, heating power, and  $\delta(x-x_0)$  is the Dirac delta function. It has a value 1 at our desired point ( $x_0$ ), and at all other points, its value is 0. That's why it allows depositing total heating power at the tumor site. Where  $x_0$  is the distance of tumor site from the skin surface. Here we consider the distance of the tumor site from the skin surface is 21 mm ( $x_0$ ). In this case, convection boundary condition is applied ( $h_f=100 \text{ W}/(\text{m}^2\cdot^\circ\text{C})$  and  $T_f=15^\circ\text{C}$ ) at the skin surface.

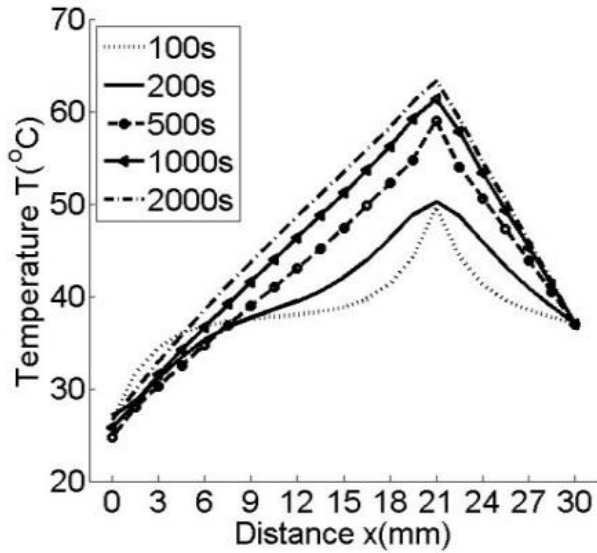


Fig. 10 Impact of point heating on tissue temperature distribution.

In Fig. 10, temperature distribution at different times is shown where point heating with a point heat source of  $P_1(t)=2500 \text{ W}/\text{m}^2$  is applied. This figure demonstrates that due to point heat source, the position of the maximum temperature remains constant at the site of the point source at different times.

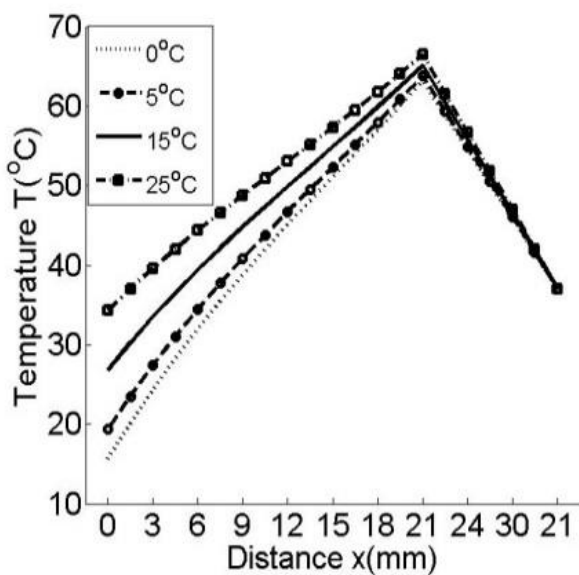


Fig. 11 Influence of cooling medium temperature to steady state temperature distribution.

In Fig. 11 the temperature response under different temperatures of cooling fluid is analysed where in Fig. 12 influence of tissue temperature under different heating power is shown. Both results are computed for the steady state condition. In Fig. 11, point source of  $P_1(t)=2500 \text{ W}/\text{m}^2$  is used. Fig. 11 shows that the magnitude and position of the highest steady state temperature are changeless at different cooling medium temperature. It reduces skin surface temperature considerably.

From Fig. 12 it is clear that higher power of the point heat leads to a higher temperature. Moreover, tissue temperature sensitivity due to point heating power decreases along with the distance from point heat source.

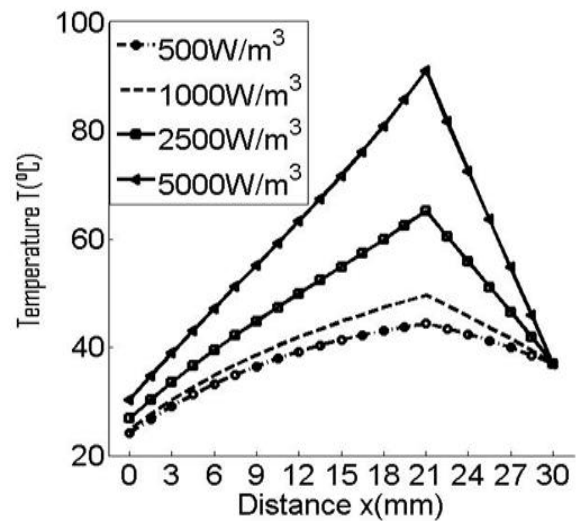


Fig. 12 Impact of point heating power on steady state temperature distribution.

### 3.8 Tissue Temperature Fluctuation under Stochastic Cooling Medium Temperature

Earlier, we consider the surrounding fluid temperature as constant. However, practically surrounding fluid temperature does not remain constant; rather, it fluctuates over time. So it is necessary to know the impact of such stochastic behavior. For this purpose, we use the following expression for flowing medium temperature.

$$T_e = T_f + \varepsilon(t) \tag{16}$$

Where  $\varepsilon(t)$  the stochastic variance in  $T_e$  and  $T_f$  is the equilibrium value if the environmental temperature. This variance gives the environmental temperature a stochastic value. We assume

$$\varepsilon_t = \lambda_t(0.05 - \sigma_i) \tag{17}$$

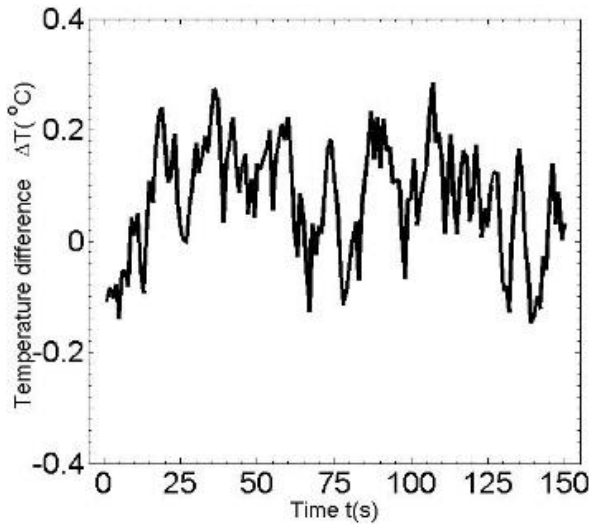
Where  $\varepsilon$  and  $t$  is the stochastic variance in environmental temperature and the discrete-time, respectively;  $\sigma_i$  is the random number between 0 and 1.

Fig. 13 and Fig. 14 depict the influences of variance in environmental temperature with different convection coefficient between the cooling medium and skin surface. Fig.

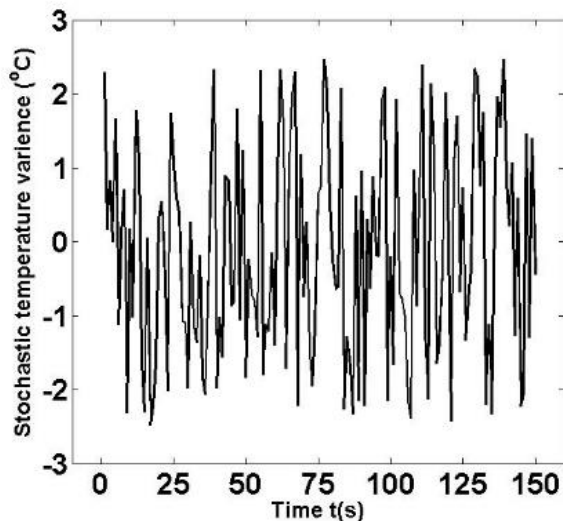
13 (a) and Fig. 14 (a) shows the tissue temperature fluctuation over time where Fig. 13 (b) and Fig. 14 (b) shows the fluctuation of stochastic variance. These figures demonstrate that due to irregular cooling medium temperature, the tissue temperature fluctuates within a certain range. Moreover, the frequency of the tissue temperature is much smaller than that of the stochastic variance. It may be noticed that as convection coefficient gets larger the temperature fluctuation magnitude also increases slightly.

Where  $Q'_m(t)$  is the stochastic variance in metabolic rate, and in the initial state, the metabolic rate was considered as constant  $Q_M$ . Here we assumed that

$$Q'_m(t) = \lambda_q(0.5 - \sigma_i) \tag{19}$$

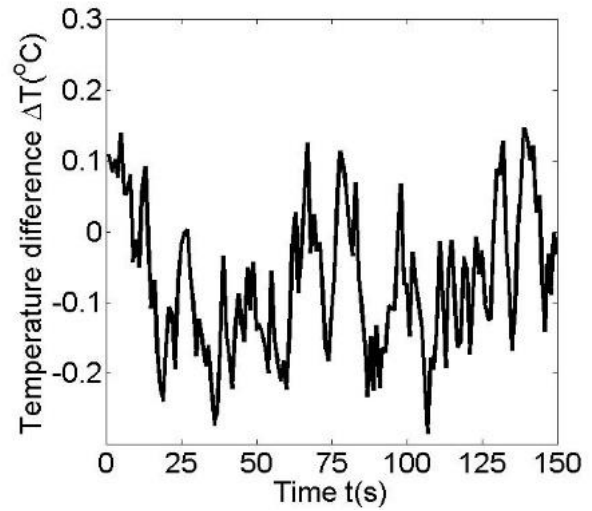


(a)

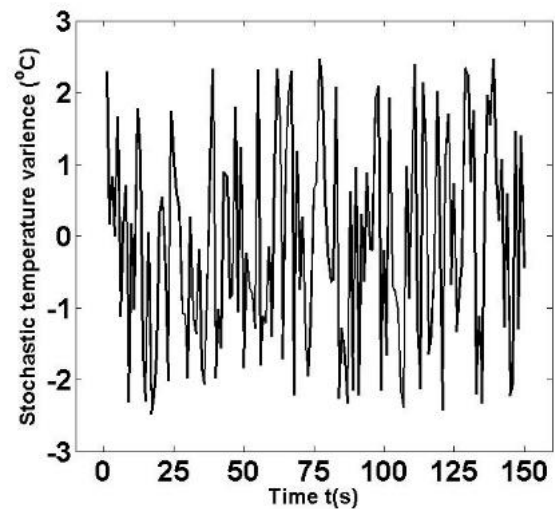


(b)

Fig. 13 Impact of stochastic temperature variance on tissue temperature ( $h_f=100 \text{ Wm}^{-2}$ ).



(a)



(b)

Fig. 14 Impact of stochastic temperature variance on tissue temperature ( $h_f=25 \text{ Wm}^{-2}$ ).

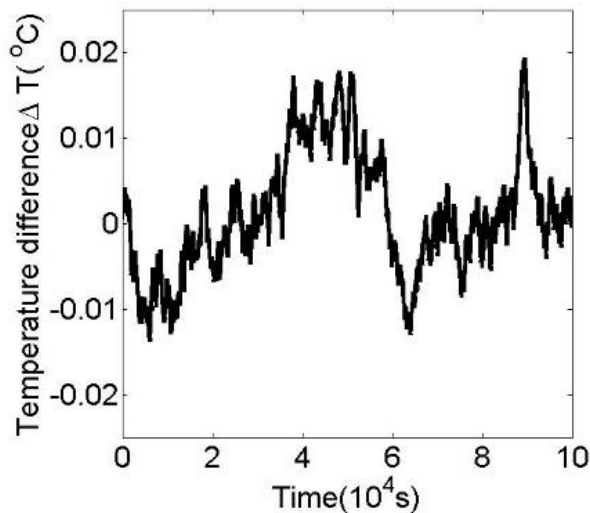
Where  $Q'_m$  and  $t$  is the stochastic variance in metabolic heat generation and the discrete-time respectively;  $\sigma_i$  the random number between 0 and 1 and  $t$  is the discrete stochastic variance in environmental temperature. And  $\lambda_q$  is a constant, which was regarded as  $Q_m/10$  in this study.

### 3.9 Tissue Temperature Fluctuation Due to Stochastic Heating

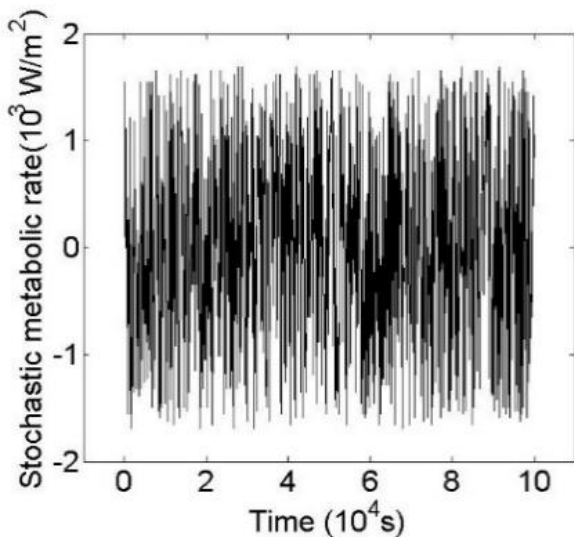
In this section, we will analyze about stochastic heating, which may be encountered for biological rhythm or stochastic external heating in hyperthermia treatment. This case corresponds to the spatial heating of the following type.

$$Q_f = Q'_m(t) \tag{18}$$

The calculated results are shown in Fig. 15 which indicates that due to stochastic heating the temperature fluctuates within a small range  $\pm 0.1$ . Fig. 15 (a) shows the tissue temperature fluctuation over time where Fig. 15 (b) shows the fluctuation of stochastic variance. Section 4.8 and Section 4.9 clearly indicates that the biological body, tends to keep its temperature balance.



(a)



(b)

**Fig. 15** Influence of variance in metabolic rate on tissue temperature.

#### 4. Summary

In this paper, a one dimensional Finite Element Model was developed to know the temperature profile inside the human tissue subject to numerous heating pattern i.e., spatial heating, surface heating, point heating, and stochastic heating. Effect of heating frequency, blood perfusion, and scattering coefficient are also discussed briefly. Which can be used in parameter estimation. It is found that for destroying a target cell point, heating is more suitable than other heating as it increases the temperature of the target region, and it has a relatively low impact on nearby unaffected cells. Moreover, a higher scattering coefficient leads to a higher temperature, where higher blood perfusion leads to lower temperature. As heating apparatus such as laser or microwave may have different power and scattering coefficient. The results obtained in this paper can be used to select a suitable apparatus. During treatment, fluctuation of environmental fluid temperature may be out of consideration as its impact on tissue temperature is almost negligible, as shown in stochastic heating. The different heating

styles used for investigation in this study are generally carried out in clinical trials. Hence results described in this paper could be beneficial to predict the treatment outcome before the treatment. This will help to detect the possible risk as well as increasing the effectiveness of the treatment. Moreover, the developed Finite Element Model and computer code can be further use to solve more practical bio-heat transfer problems.

#### References

- [1] Kasevich, R.S., McQueeney, J.F. and Crooker, R.H., KASEVICH ASSOC Inc, 1988. *Method and apparatus for hyperthermia treatment*. U.S. Patent 4,776,086.
- [2] Khanafer, K. and Vafai, K., 2009. Synthesis of mathematical models representing bioheat transport. *Advances in numerical heat transfer*, 3, pp.1-28.
- [3] Pennes, H.H., 1948. Analysis of tissue and arterial blood temperatures in the resting human forearm. *Journal of applied physiology*, 1(2), pp.93-122.
- [4] Shih, T.C., Yuan, P., Lin, W.L. and Kou, H.S., 2007. Analytical analysis of the Pennes bioheat transfer equation with sinusoidal heat flux condition on skin surface. *Medical Engineering & Physics*, 29(9), pp.946-953.
- [5] Shen, W., Zhang, J. and Yang, F., 2005. Modeling and numerical simulation of bioheat transfer and biomechanics in soft tissue. *Mathematical and Computer Modelling*, 41(11-12), pp.1251-1265.
- [6] Xu, F., Lu, T.J. and Seffen, K.A., 2008. Biothermomechanical behavior of skin tissue. *Acta Mechanica Sinica*, 24(1), pp.1-23.
- [7] Deng, Z.S. and Liu, J., 2002. Monte Carlo method to solve multidimensional bioheat transfer problem. *Numerical Heat Transfer: Part B: Fundamentals*, 42(6), pp.543-567.
- [8] Ooi, E.H. and Ang, W.T., 2008. A boundary element model of the human eye undergoing laser thermokeratoplasty. *Computers in Biology and Medicine*, 38(6), pp.727-737.
- [9] Ooi, E.H., Ang, W.T. and Ng, E.Y.K., 2007. Bioheat transfer in the human eye: a boundary element approach. *Engineering Analysis with Boundary Elements*, 31(6), pp.494-500.
- [10] Hwang, S.C. and Lemmonier, D., 1970. Coupling numerical solution of bio-heat transfer equation and Maxwell's equations in biological tissues during hyperthermia. *WIT Transactions on Biomedicine and Health*, 2.
- [11] Reddy, J. N., 2006. *An Introduction to the Finite Element Method*, 3rd edition, McGraw Hill, Inc.
- [12] Deng, Z.S. and Liu, J., 2002. Analytical study on bioheat transfer problems with spatial or transient heating on skin surface or inside biological bodies. *J. Biomech. Eng.*, 124(6), pp.638-649.
- [13] Karaa, S., Zhang, J. and Yang, F., 2005. A numerical study of a 3D bioheat transfer problem with different spatial heating. *Mathematics and Computers in simulation*, 68(4), pp.375-388.
- [14] Sardari, D. and Verga, N., 2011. *Cancer treatment with hyperthermia*. INTECH Open Access Publisher.
- [15] Cheung, A.Y. and Neyzari, A., 1984. Deep local hyperthermia for cancer therapy: external electromagnetic and ultrasound techniques. *Cancer Research*, 44(10 Supplement), pp.4736s-4744s.